ANNALS of Clinical and Translational Neurology
Open Access
ANA American Neurological Association since 1875

RESEARCH ARTICLE

Brain atrophy measures in preclinical and manifest spinocerebellar ataxia type 2

Kathrin Reetz[1,2], Roberto Rodríguez-Labrada[3], Imis Dogan[1,2], Shahram Mirzazade[1,2], Sandro Romanzetti[1,2], Jörg B. Schulz[1,2], Edilia M. Cruz-Rivas[4], Jose A. Alvarez-Cuesta[4], Raul Aguilera Rodríguez[3], Yanetza Gonzalez Zaldivar[5], Georg Auburger[6] & Luis Velázquez-Pérez[3]

[1]Department of Neurology, RWTH Aachen University, Pauwelsstr. 30, 52074 Aachen, Germany
[2]JARA-BRAIN Institute Molecular Neuroscience and Neuroimaging, Forschungszentrum Jülich GmbH and RWTH Aachen University, 52074 Aachen, Germany
[3]Department Clinical Neurophysiology, Centre for the Research and Rehabilitation of Hereditary Ataxias, Calle Libertad 26, Holguín 80100, Cuba
[4]Department of Imaging, Clinical-Surgical Hospital "Lucía Iñiguez". Avenue "Celia, Sanchez 1, Holguín, Cuba
[5]Department Molecular Genetics, Centre for the Research and Rehabilitation of Hereditary Ataxias, Calle Libertad 26, Holguín 80100, Cuba
[6]Experimental Neurology, Goethe University Medical School, 60590 Frankfurt/Main, Germany

Correspondence
Luis Velázquez-Pérez, Centre for the Research and Rehabilitation of Hereditary Ataxias, Calle Libertad 26, Holguín 80100, Cuba. Tel: 53 24 462823; Fax: 53 24 481517;
E-mail: velazq63@gmail.com

Funding Information
KR was funded partly by the Excellence Initiative of the German federal and state governments, and the Federal Ministry of Education and Research (BMBF 01GQ1402 to KR). LV was funded partly by a Georg Forster Research Award from the Alexander von Humboldt Foundation and the Cuban Ministry of Public Health. The funders had no role in the present study.

Received: 11 August 2017; Revised: 6 October 2017; Accepted: 21 October 2017

doi: 10.1002/acn3.504

Abstract

Objective: Spinocerebellar ataxia type 2 (SCA2) is an autosomal dominantly inherited neurodegenerative disease mainly affecting the cerebellum and brainstem. In this Cuban-German research collaboration, we aimed to characterize atrophy patterns and associations with clinical measures in preclinical and manifest SCA2. **Methods**: In this study, 16 nonmanifest SCA2 mutation carriers, 26 manifest patients with SCA2, and 18 healthy control subjects underwent magnetic resonance imaging, as well as genetic and clinical characterization including assessment of ataxia (Scale for the Assessment and Rating of Ataxia) and saccade velocity in Cuba were enrolled. Semiautomated quantitative volumetry of the cerebellum and brainstem, subdivided into the medulla oblongata, the pontine brainstem, and mesencephalon was performed. Additionally, the anteroposterior diameter of the pontine brainstem was measured. **Results**: Analysis of volumetric data revealed degeneration of the cerebellum and brainstem, in particular of pontine volumes and the anteroposterior diameter of the pons, in both manifest SCA2 patients and individuals at risk for SCA2 compared to controls. Comparing patients with nonataxic preclinical SCA2 mutation carriers, we found more pronounced reductions of the pontine brainstem and cerebellum in manifest SCA2. Volumetric data further showed associations with CAG repeat length and predicted age of onset in preclinical SCA2 individuals, and by trend with ataxia signs in patients. Although saccade velocity was associated with reduction in the pontine brainstem in preclinical and manifest SCA2, reduced ability to suppress interfering stimuli measured by the Stroop task was related to cerebellar volume loss in patients. **Interpretation**: Preclinical SCA2 mutation carriers exhibit brain abnormalities, which could be targeted as surrogate parameters for disease progression and in future preventive trials.

Introduction

Spinocerebellar ataxia type 2 (SCA2) is an autosomal dominantly inherited disease caused by the abnormal expansion of cytosine–adenine–guanine (CAG) triplet repeats in the encoding region of the *ATXN2* gene.[1] Clinically, SCA2 is characterized by gait ataxia, cerebellar dysarthria, dysmetria, and dysdiadochokinesia; features that can be accompanied by slowing of horizontal saccadic eye movements, peripheral neuropathy, dysautonomic disorders, cognitive dysfunction, sleep disturbances, and signs of motor neuron involvement.[2,3] Symptoms typically occur by the third or fourth decade in life. Although clinical trials are emerging,[4] up-to-date,

no effective treatment is available. Worldwide, SCA2 is the second most frequent type of spinocerebellar ataxia, only surpassed by SCA3. In Holguín, Cuba, the disease reaches the highest prevalence, resulting from a putative founder effect.[3]

Neuropathological studies have shown progressive neuronal death of Purkinje cells in the cerebellum and several pontine, mesencephalic, and thalamic neurons among other cells resulting in a reduction of overall brain size with significant atrophy of the cerebellum, brainstem, and frontal lobe.[5] Magnetic resonance imaging (MRI) data are sparse and often comprise only small sample sizes in this orphan disease. The available structural MRI data have so far confirmed the neuropathological findings showing atrophy of the brainstem and cerebellum,[6–8] but there is also some evidence for cortical brain atrophy and microstructural abnormalities in SCA2 patients.[9–13] For preclinical SCA2 mutation carriers, only two structural MRI studies exist. The Ataxia Study Group (www.ataxia-study-group.net) investigates the natural history of the preclinical stages in SCA1, SCA2, SCA3, and SCA6 (RISCA). Here, although sample size was limited to four preclinical SCA2 mutation carriers, we were able to report loss of volume in the brainstem and cerebellum compared to noncarriers.[14] In a larger sample from Cuba, manual volumetric delineation displayed mild cerebellar and pontine atrophy in some cases.[15] Given the limited data on MRI biomarker, this Cuban-German collaboration is the first and largest study investigating preclinical and manifest SCA2 mutation carriers compared to controls using quantitative volumetry (1) to distinguish structural changes in the brainstem and the cerebellum at different stages of the disease and (2) to identify genetic and clinical relations with neurodegeneration.

Materials and Methods

Participants and procedures

This study enrolled in total 60 subjects, including 16 nonataxic SCA2 mutation carriers (27–64 years of age) and 26 manifest SCA2 patients (18–59 years), who were compared to a group of 18 healthy controls (14–71 years) with no history of neurologic or psychiatric disorders (Table 1). Groups did not significantly differ with respect to age ($F_{2,57} = 1.4$, $P = 0.255$) or sex ($\chi^2 = 3.794$, $P = 0.150$). CAG repeat length was overall higher in manifest SCA2 (range from 32 to 55 CAG repeats) compared to preclinical individuals at risk (32–40; Mann–Whitney $U = 93.5$, $z = -3.0$, $P = 0.002$). Age of onset was estimated in preclinical SCA2 from the number of CAG repeats within the range of 34–45 using a survival analysis model obtained in a large population of 924 Cuban SCA2 patients and nonataxic carriers,[16] and in two subjects with 32 and 33 CAG repeats according to the formula by Pulst et al.[1] Disease duration in patients and estimated time to manifestation in preclinical SCA2 were calculated based on subjects' age at study participation and [predicted] age of onset.

Clinical cerebellar signs were evaluated using the Scale for the Assessment and Rating of Ataxia (SARA)[17] ranging from 0 to 2 in preclinical SCA2 and from 6 to 32 in SCA2 patients. The Stroop Color-Word Interference test[18] including a color naming and interference condition was used to assess selective attention and the ability to suppress interfering stimuli. The analyzed parameter was the corrected time of interference task, i.e., time needed for the color naming condition subtracted from the interference condition, to ensure that frontal lobe function adjusted for potential saccadic impairments in SCA2 was measured. Finally, horizontal saccades were recorded binocularly with a 2-channel Otoscreen AC electrooculography (EOG) (Jaeger-Toennies, 97204 Höchberg, Germany), using silver-silver chloride electrodes over right and left outer canthus of the eyes. Saccades were triggered by a circular white target on a black background, subtending an angle of 0.7 degrees. The EOG signal was amplified and bandpass filtered (0.2–70 Hz). The data were sampled at a frequency of 200 Hz with a time base of 1000 msec/division, sensitivity of 200 μV/division and a time constant of 8 sec. Subjects were asked to fixate the target in the central position and to redirect their gaze to the new location of the target as soon as it appeared in the periphery, and later back in the central position. A total of 10 centrifugal saccades in left and right directions were registered for 60° predictable amplitudes. Before and after all recordings, EOG signals were calibrated for a horizontal angle of 30°. Maximal saccade velocity was obtained through the automated data analysis software contained in the Otoscreen package.

This study was approved by the Ethics Committee of the Center for the Research and Rehabilitation of Hereditary Ataxias (Holguín, Cuba) and was conducted according to the Declaration of Helsinki. Each subject gave written informed consent for participation in the study.

Magnetic resonance imaging

Subjects underwent MR imaging in Holguín, Cuba (Department of Imaging, Clinical-Surgical Hospital "Lucía Iñiguez") on a 0.23 T scanner (Philips, Tokyo, Japan). The MR image protocol included 51 transversal, 7 coronal, and 2 sagittal spin-echo T1-weighted images (section thickness, 5 mm; TR = 24 msec; TE = 9 msec). Manual delineation and segmentation of brainstem structures and the cerebellum in pseudonymized images were performed

by SM, who is highly experienced in manual volumetric techniques,[19] using the open-source software ITK-SNAP version 2.4.0.[20] The following volumes were measured: the total cerebellum, the total brainstem. and brainstem regions subdivided into the midbrain, pontine brainstem, and medulla oblongata (Fig. 1). Additionally, we measured the anterior–posterior diameter of the pontine brainstem perpendicular to the pontine brainstem axis using sagittal T1-weighted images (Fig. 1A). As some scans had no full coverage of the entire brain (seven controls, seven preclinical SCA2 and 14 patients), the total intracranial volume (TICV) was estimated using the

Table 1. Demographics and clinical characteristics of the study population.

	Manifest SCA2 (n = 26) Mean ±SD	Preclinical SCA2 (n = 16) Mean ±SD	Controls (n = 18) Mean ±SD	P
Age (years)	42.2 ± 10.3	40.2 ± 8.4	36.8 ± 12.5	0.255[1]
Gender (female/male)	10/16	11/5	10/8	0.150[2]
CAG repeat lengths	39.6 ± 4.4	36.1 ± 2.3	n.a.	0.002
Age of onset (years)	32.1 ± 9.4	53.3 ± 11.2[3]	n.a.	<0.001
Disease duration (years)	10.1 ± 5.7	−13.1 ± 8.7[4]	n.a.	
SARA total score	14.5 ± 6.1	0.8 ± 0.9	n.a.	
Maximal saccade velocity (°/sec)	294.0 ± 141.9	374.0 ± 110.7	n.a	0.061
Stroop interference task* (sec)	55.9 ± 47.03	46.8 ± 22.2	n.a	0.475

SD, standard deviation; SARA, Scale for the Assessment and Rating for Ataxia; n.a., not applicable; °, angle; *corrected for color naming condition. p: p-value from [1]ANOVA, [2]Chi-square test (remaining group comparisons assessed with Mann–Whitney U-tests); [3]estimated age of onset, calculated according to Almaguer-Mederos et al. (2010) or Pulst et al. (1996); [4]time to manifestation [age – estimated age of onset].

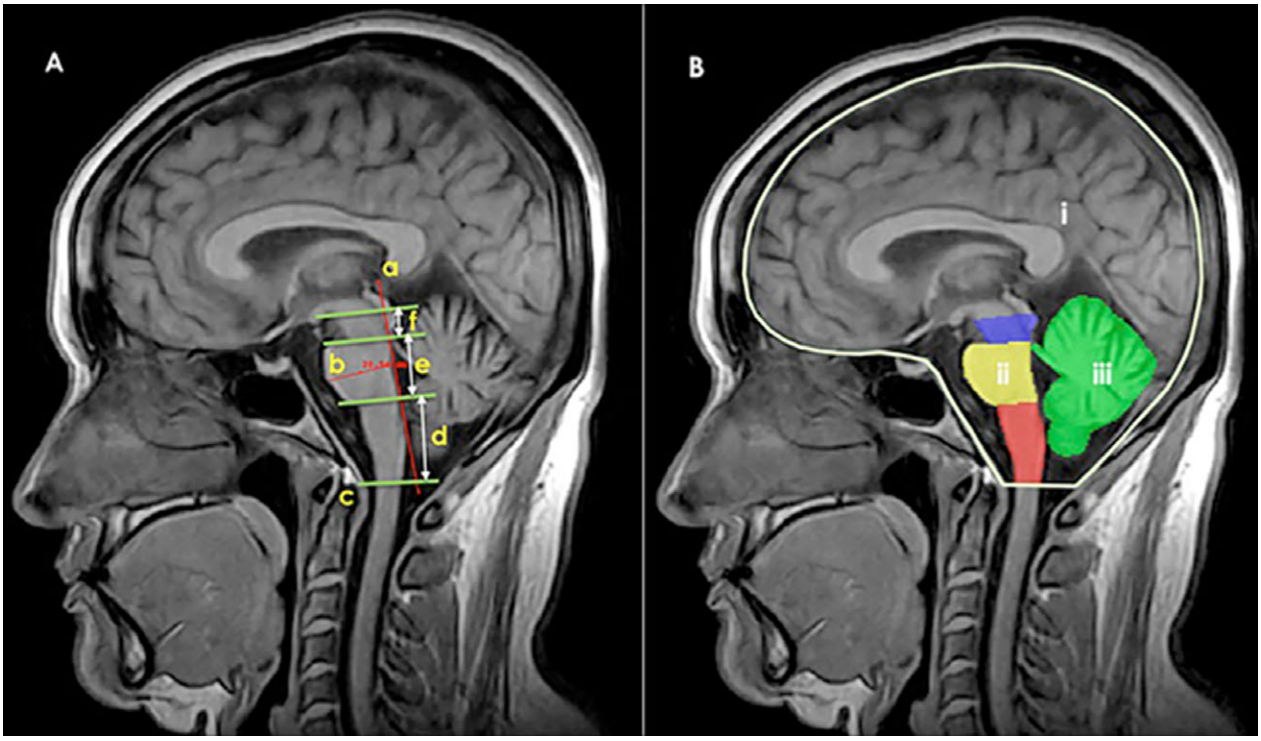

Figure 1. (A) Definition of distances and boundaries for manual segmentation: (a) line along the tangent to the pontine brainstem (rostral–caudal), (b) pontine brainstem diameter at the level of opening of the sella turcica perpendicular to line a, (c) lowest border of brainstem delimited on the plan-line along the foramen magnum, (d) area of the medulla (defined between level of foramen magnum and pontine brainstem), (e) area of the pontine brainstem (defined between mesencephalon and myelencephalon), and (f) area of the midbrain (defined between cranial border of pontine brainstem and pontine brainstem body). (B) Shows the quantitatively measured regions: (i) total intracranial volume [TICV], (ii) brainstem including mesencephalon in blue, pontine brainstem in yellow, medulla oblongata in red, and (iii) cerebellum in green.

following procedure: First, the available brain volumes were manually segmented in subject space using ITK-SNAP and then normalized to the Montreal Neurological Institute (MNI) template using SPM12 (http://www.fil.ion.ucl.ac.uk/spm/). Each normalized image was then projected to the MNI template mask in order to calculate the percentage of missing voxels for each subject. Here, the individual TICV derived from manual segmentation using ITK-SNAP for each subject were then adjusted for missing brain portions resulting in an estimation of TICV for the entire brain.

Statistical analysis

For statistical comparisons, volumes of the total brainstem, mesencephalon, pontine brainstem, medulla and cerebellum were normalized to the TICV, expressed as percentage (%TICV). Group differences in volumetric data were tested using Kruskal–Wallis tests, followed by pairwise comparisons using Mann–Whitney U-tests (one-tailed, Bonferroni corrected for multiple comparisons). We report effect size estimates r for group differences calculated from z-scores divided by the number of observations[21] where $r > 0.3$ is considered as medium and >0.5 as large effect sizes. Finally, we used Spearman's rho r_s to investigate associations between brain volumes and genetic (CAG repeats) or clinical features (i.e., age of onset and disease duration in patients, predicted age of onset and inverse time to manifestation in preclinical SCA2, maximal saccade velocity, and corrected time of Stroop interference task) for each group separately. Correlations with SARA scores were calculated for patients only. Note that due to the exploratory investigation of associations between brain volumes and clinical measure, correlations were not adjusted for multiple testing (uncorrected p-values, two-tailed). All statistical analyses were performed using SPSS version 21 (IBM) with an alpha set at 0.05 as the statistical threshold for significance.

Results

Volumes of the pontine brainstem and mesencephalon were available in all 60 subjects, whereas the medulla and cerebellum could not be completely segmented in 13 and 18 subjects, respectively. In total, analysis of the brainstem and medulla included 13 controls, 12 preclinical SCA2, and 22 manifest patients; data on cerebellar volumes were available in 17 patients (Table 2).

Except for TICV and medulla, we found significant group differences for all remaining volumes (Figure 2, Table 2). Compared to the control group, both brainstem and cerebellar volumes were reduced in manifest patients with large effect sizes ($U = 20$, $z = -4.199$, $P < 0.0001$, $r = -0.71$ and $U = 1$, $z = -4.583$, $P < 0.0001$, $r = -0.84$, respectively), and with medium effect sizes in preclinical SCA2 ($U = 32$, $z = -2.502$, $P = 0.018$, $r = -0.50$ and U = 35, $z = -2.339$, $P = 0.027$, $r = -0.47$, respectively). Cerebellar volumes were also significantly lower in manifest compared to preclinical SCA2 ($U = 32$, $z = -3.1$, $P = 0.003$, $r = -0.58$), whereas for the brainstem the medium-sized difference did not survive Bonferroni adjustment for multiple comparisons ($U = 81$, $z = -1.838$, $P = 0.102$, $r = -0.32$). However, within the brainstem, in particular, pontine volume loss was observed in manifest patients ($U = 21$, $z = -5.084$, $P < 0.0001$, $r = -0.77$) and nonataxic mutation carriers ($U = 60$, $z = -2.898$, $P = 0.006$, $r = -0.50$) compared to controls, and importantly in manifest compared to preclinical SCA2 showing a large effect size ($U = 65$, $z = -3.704$,

Table 2. Volumetric results in SCA2 and controls.

	Manifest SCA2			Preclinical SCA2			Controls			
	n	Median[IQR]	*r*	*n*	Median[IQR]	*r*	*n*	Median[IQR]	*r*	*P*
TICV (liter)	26	1.47 [1.33; 1.58]	−0.09	16	1.41 [1.33; 1.52]	−0.11	18	1.47 [1.38; 1.60]	−0.22	0.452
Brainstem (% TICV)	22	1.27 [1.14; 1.45]**	−0.71	12	1.48 [1.22; 1.62]	−0.32	13	1.65 [1.59; 1.78]*	−0.50	<0.0001
Mesencephalon (% TICV)	26	0.41 [0.34; 0.52]¶	−0.30	16	0.39 [0.37; 0.43]	−0.06	18	0.47 [0.41; 0.58]*	−0.44	0.034
Pons (% TICV)	26	0.52 [0.49; 0.60]**	−0.77	16	0.74 [0.65; 0.85]**	−0.57	18	0.91 [0.83; 1.02]*	−0.50	<0.0001
Medulla (% TICV)	22	0.24 [0.21; 0.32]	−0.12	12	0.27 [0.24; 0.28]	−0.19	13	0.26 [0.23; 0.28]	−0.04	0.543
Cerebellum (% TICV)	17	5.66 [4.92; 6.15]**	−0.84	12	6.67 [6.43; 7.34]*	−0.58	13	7.57 [6.80; 8.33]*	−0.47	<0.0001
Anteroposterior diameter of the pons (mm)	26	17.2 [16.2; 19.6]**	−0.78	16	20.9 [19.4; 22.6]**	−0.54	18	23.4 [23.0; 23.8]*	−0.53	<0.0001

TICV, total intracranial volume; volumes are expressed as percentage of the total intracranial volume (% TICV); IQR, interquartile range; *r*: effect size estimate for group differences compared to previous group (in manifest SCA2 compared to controls); *p*: p-value from Kruskal–Wallis test; pairwise comparisons (Mann–Whitney U-tests, corrected for multiple comparisons): *significant difference compared to previous group (in manifest SCA2 compared to controls) at $P < 0.05$ or **$P < 0.0001$; ¶difference compared to controls did not survive Bonferroni correction ($P = 0.069$).

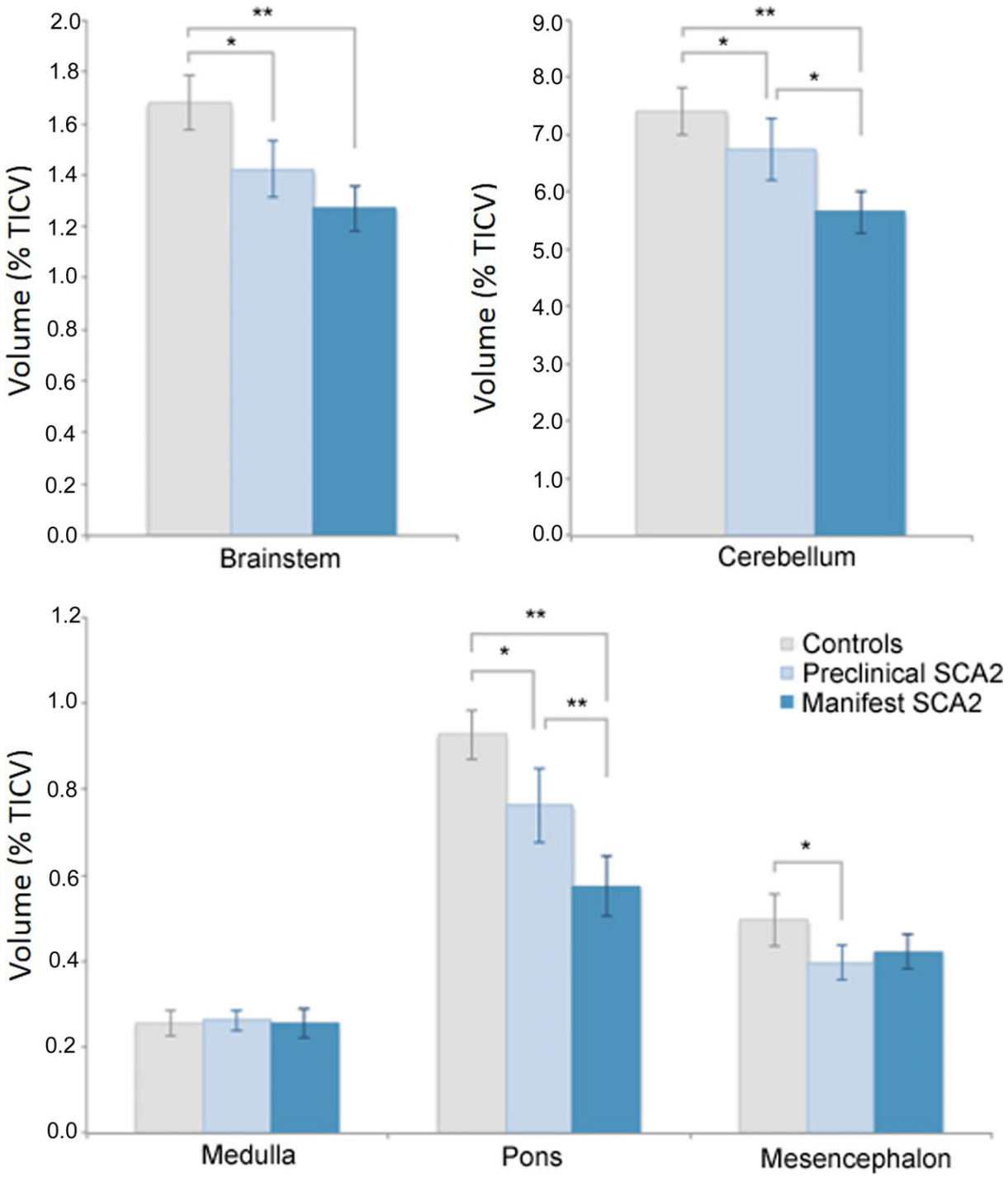

Figure 2. Volumetric results of (A) brainstem, (B) cerebellum, and (C) brainstem structures in SCA2 and controls. Volumes are expressed as percentage of the total intracranial volume (TICV). Data are means and 95% confidence intervals (error bars). Asterisks indicate significant differences between groups at $*P < 0.05$ or $**P < 0.0001$ (Bonferroni corrected for multiple comparisons).

$P < 0.0001$, $r = -0.57$). Midbrain volume loss was only observed for preclinical SCA2 compared to controls ($U = 70$, $z = -2.553$, $P = 0.015$, $r = -0.44$), while volume differences between patients and controls marginally failed to reach significance after correction for multiple comparisons ($U = 150$, $z = -2.005$, $P = 0.069$, $r = -0.30$).

We additionally measured the anteroposterior diameter of the pontine brainstem. Compared to controls, the anteroposterior diameter showed significant reductions of large effect sizes in patients ($U = 17$, $z = -5.2$, $P < 0.0001$, $r = -0.78$) and preclinical SCA2 ($U = 54$, $z = -3.1$, $P = 0.003$, $r = -0.53$), as well as in manifest compared to preclinical SCA2 ($U = 74$, $z = -3.5$, $P < 0.0001$, $r = -0.54$).

Correlation analyses in preclinical SCA2 showed that CAG repeat length was inversely correlated with volumes of the brainstem ($r_s = -0.639$, $P = 0.025$; Fig. 3A), medulla ($r_s = -0.657$, $P = 0.02$), pontine brainstem ($r_s = -0.526$, $P = 0.036$; Fig. 3B), and cerebellum ($r_s = -0.712$, $P = 0.009$; Fig. 3C). Estimated age of onset in preclinical SCA2 showed a positive correlation with volumes of the medulla ($r_s = 0.647$, $P = 0.023$), and a trend for an association with the anteroposterior diameter of the pontine brainstem ($r_s = 0.485$, $P = 0.057$) and pontine volumes ($r_s = 0.428$, $P = 0.098$). In manifest SCA2 patients, SARA scores were by trend related to reduced brainstem volumes ($r_s = -0.372$, $P = 0.089$; Fig. 3D). Maximal saccade velocity was correlated with volumes of the pontine brainstem both in preclinical SCA2 ($r_s = 0.559$, $P = 0.024$) and in manifest SCA2 ($r_s = 0.456$, $P = 0.019$; Fig. 3E), and by trend in preclinical SCA2 with volumes of the brainstem ($r_s = 0.510$, $P = 0.090$) and medulla ($r_s = 0.550$, $P = 0.067$). In addition, maximal saccade velocity was correlated with the anterior–posterior diameter of the pontine brainstem in both groups (preclinical SCA2; $r_s = 0.550$ $P = 0.027$; manifest SCA2; $r_s = 0.387$, $P = 0.048$). Corrected time of Stroop interference performance in SCA2 patients showed an inverse correlation with cerebellar volumes ($r_s = -0.596$, $P = 0.012$, Figure 3F).

Discussion

This imaging study provides quantitative measurements of brain volumes in the rare neurodegenerative disease SCA2. In this so far largest sample of preclinical and manifest SCA2 Cuban mutation carriers, we performed quantitative manual segmentation and volumetry of the brainstem and cerebellum, and measured the anterior–posterior diameter of the pontine brainstem. Our major finding is that both brainstem, in particular pontine, and cerebellar volumes are reduced in manifest and already in preclinical SCA2 mutation carriers showing medium to large effect sizes compared to controls. Importantly, atrophy of the pontine brainstem and cerebellum was more pronounced in the manifest compared to the preclinical stage with large effect sizes, indicating that measurements of pontine and cerebellar volumes differentiate between clinical stages and may qualify as a potential biomarker to monitor disease progression. Also, a medium-sized effect was observed for total brainstem atrophy in manifest compared to preclinical SCA2 mutation carriers, which, however, was not statistically significant. Given that the midbrain and medulla did not show differences between premanifest and manifest SCA2, in spite of their well-documented pathology in the course of SCA2,[22,23] total brainstem measurements may therefore lack sensitivity to distinguish between disease stages and thus, pontine measures should be preferred. Finally, we found correlations of volumetric data with CAG repeat length and predicted age of onset in preclinical SCA2 mutation carriers, and with Stroop interference task and by trend with ataxia signs measured by the SARA in SCA2 patients. Slowing of saccade velocity was related to pontine atrophy in both disease stages.

Our results confirm previous neuropathological[5] and imaging data[24,25] in manifest SCA2 mutation carriers and can be regarded as highly valuable in preclinical SCA2 mutation carriers, as data are extremely limited. Previous manual measurements in preclinical SCA2 mutation carriers revealed light cerebellar atrophy in 62.5% and pontine atrophy in 29.2% of cases.[15] Compared to controls, diameters of the pontine brainstem and areas of the cerebellar vermis and hemisphere were reduced.[15] However, no quantitative comparisons between preclinical SCA2 mutation carriers and SCA2 patients were available so far. Only in comparison to noncarriers and in a very small sample, we were previously able to report loss of total brainstem volumes and gray matter in the cerebellum in preclinical SCA2 mutation carriers.[14]

MR spectroscopy in SCA2 patients further underline the neuropathological role of these disease-specific regions, showing changes of the neurochemical profile in the cerebellum und pons.[26,27] Similarly, microstructural abnormalities measured by diffusion weighted imaging have been detected in the cerebellum and the pons[28] as well as cortical alterations in SCA2 patients.[10,11,29] Functional MRI in resting-state modus further shows changes of cerebellar but also fronto- and parietal connectivity networks related to cognitive and motor performance.[30,31] No multimodal MRI data other than macroanatomical measurements exist for the preclinical stage of the disease. However, given the already measurable structural changes in nonataxic mutation carriers further assessments of early microstructural and functional alterations would be highly desirable. Prospective, longitudinal studies, as shown for other spinocerebellar diseases such as SCA1, SCA3, and SCA6, will be needed to measure rates of progression[19] that can be used to monitor treatment effects in clinical trials.

Atrophy of the cerebellum, brainstem, and pons was linked to the number of CAG repeats in preclinical SCA2

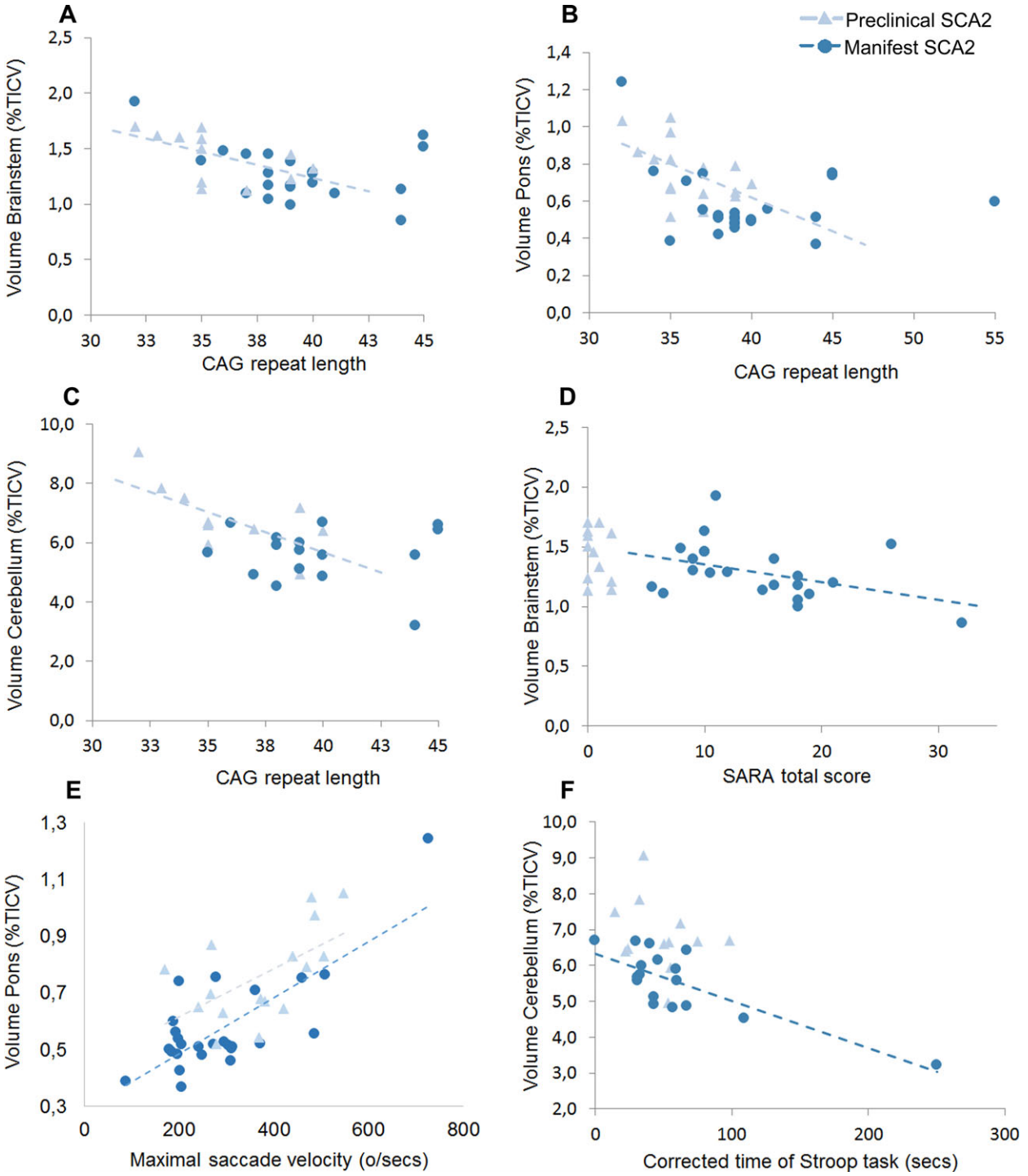

Figure 3. Scatter plots demonstrating significant correlations (at $P < 0.05$) between CAG repeat length and volumes of the (A) brainstem, (B) pontine brainstem, and (C) cerebellum in preclinical SCA2; (D) in manifest SCA2 patients SARA scores and brainstem volumes were associated only by trend ($r_s = -0.372$, $P = 0.089$); (E) Maximal saccade velocity was correlated with volumes of the pontine brainstem both in preclinical SCA2 and in manifest SCA2; (F) Stroop interference performance (corrected for color naming) correlated with cerebellar volumes in SCA2 patients. Volumes are expressed as percentage of the total intracranial volume (%TICV); triangles represent preclinical SCA2, circles manifest SCA2 patients; trend line indicates the direction of the association.

individuals, and earlier predicted age of onset was by trend related to reduced volumes of the pons. In the manifest stage, we could not detect any correlations of volumetric changes with genetics, disease duration or age of onset. As CAG repeat length is inversely correlated with age of onset,[1,16] this might indicate that genetic load plays a role in the early degenerative process, but may have no additional impact on volumetric changes in the manifest stage. In patients, we only observed a medium-sized, albeit non-significant, association between SARA scores and reduced brainstem volumes. Although SARA assesses progression of cerebellar ataxia signs, this finding points to the potential clinical linkage of our volumetric findings.

In this context, the crucial role of the pontine brainstem in the neurodegenerative process in this disease is compatible with the prominent horizontal saccade slowing that SCA2 patients exhibit even before the ataxia onset,[32,33] since the horizontal saccade velocity has their main generators at pontine levels, specifically in the paramedian pontine reticular formation.[34] Indeed, this notion is supported by our data showing strong correlations between pontine brainstem volumes and saccade slowing in manifest SCA2 as well as preclinical subjects. To our knowledge, this is the first work exploring the association of brain volumes and saccade velocity in SCA2. Besides, the degeneration of the pontine brainstem in SCA2 is in line with the early REM sleep pathology characterizing the disease from prodromal to manifest stage[35–37] since the neural circuit controlling this sleep stage lie mainly in the pontine brainstem.[38,39]

In the present paper, we also observed a significant association between cerebellar volumes and Stroop interference task in the manifest SCA2 group but not in the preclinical subjects. This finding supports a cerebellar contribution to executive functions such as the ability to inhibit interfering stimuli and suggests disruptions of cerebello-thalamic-cortical projections,[40] in line with the profound degeneration of the thalamus in SCA2.[41,42] In addition, previous studies in SCA2 patients demonstrated associations between cognitive function and brain imaging findings using voxel-based morphometry and resting-state functional MRI.[30,43]

This study is limited by its cross-sectional nature, and longitudinal studies are highly warranted to assess atrophy rates over time. Another limitation is that fully automated objective analysis was not possible due to the MRI assessment (e.g., low magnetic field strength, field of view). Although we aimed to avoid any analytical bias, the applied manual segmentation procedure is prone to rater bias and manual misjudgment (e.g., at structure boundaries), effects of which cannot be completely ruled out. This may in particular pertain to the somewhat contradictory results of less midbrain volume in preclinical SCA2 compared to controls, which, however, was less pronounced in the manifest stage. Using an additional approach, we measured the anterior–posterior diameter of the pontine brainstem, which overall was coherent with our data on pontine volumes and indicates plausibility of volumetric assessments. Another limitation is that we could not perform a data-driven approach across the whole-brain, but restricted our analysis to particular regions of interest known to be affected by disease pathology. Future studies with higher resolution imaging and using different MRI modalities are needed to evaluate the predictive value of whole-brain alterations for disease progression in SCA2.

Overall, our results demonstrate early neurodegenerative patterns already detectable in the preclinical stage of SCA2, indicating that the pontine brainstem and cerebellum are the most promising imaging measures to monitor disease progression in SCA2 as well as saccadic and cognitive dysfunctions.

Acknowledgments

We are grateful to the SCA2 patients, preclinical carriers, and control individuals, as well as to the Cuban Ministry of Public Health for their cooperation. KR was funded partly by the Excellence Initiative of the German federal and state governments, and the Federal Ministry of Education and Research (BMBF 01GQ1402 to KR). LV was funded partly by a Georg Forster Research Award from the Alexander von Humboldt Foundation. The funders had no role in the present study.

Author Contributions

LVP, RRL, EMCR, JAAC, RAR, and YGZ conceptualized and designed the study. KR, ID, SM, SR, LVP, RRL, EMCR, JAAC, RAR, and YGZ acquired or analyzed the data. KR, RRL, ID, SM, SR, JBS, EMCR, JAAC, RAR, YGZ, GA, and LVP drafted or revised the manuscript:.

Conflicts of Interest

The authors report no conflicts of interest that could have influenced the results of the study.

References

1. Pulst SM, Nechiporuk A, Nechiporuk T, et al. Moderate expansion of a normally biallelic trinucleotide repeat in spinocerebellar ataxia type 2. Nat Genet 1996;14:269–276.
2. Orozco Diaz G, Nodarse Fleites A, Cordoves Sagaz R, Auburger G. Autosomal dominant cerebellar ataxia: clinical analysis of 263 patients from a homogeneous population in Holguin, Cuba. Neurology 1990;40:1369–1375.

3. Velazquez Perez L, Cruz GS, Santos Falcon N, et al. Molecular epidemiology of spinocerebellar ataxias in Cuba: insights into SCA2 founder effect in Holguin. Neurosci Lett 2009;454:157–160.
4. Scoles DR, Meera P, Schneider MD, et al. Antisense oligonucleotide therapy for spinocerebellar ataxia type 2. Nature 2017;544:362–366.
5. Estrada R, Galarraga J, Orozco G, et al. Spinocerebellar ataxia 2 (SCA2): morphometric analyses in 11 autopsies. Acta Neuropathol 1999;97:306–310.
6. Klockgether T, Ludtke R, Kramer B, et al. The natural history of degenerative ataxia: a retrospective study in 466 patients. Brain 1998;121 (Pt 4):589–600.
7. Ying SH, Choi SI, Perlman SL, et al. Pontine and cerebellar atrophy correlate with clinical disability in SCA2. Neurology 2006;66:424–426.
8. Jung BC, Choi SI, Du AX, et al. MRI shows a region-specific pattern of atrophy in spinocerebellar ataxia type 2. Cerebellum 2012;11:272–279.
9. Mercadillo RE, Galvez V, Diaz R, et al. Parahippocampal gray matter alterations in Spinocerebellar Ataxia Type 2 identified by voxel based morphometry. J Neurol Sci 2014;347:50–58.
10. Hernandez-Castillo CR, Galvez V, Mercadillo R, et al. Extensive white matter alterations and its correlations with ataxia severity in SCA 2 patients. PLoS ONE 2015;10:e0135449.
11. Salvatore E, Tedeschi E, Mollica C, et al. Supratentorial and infratentorial damage in spinocerebellar ataxia 2: a diffusion-weighted MRI study. Mov Disord 2014;29:780–786.
12. Mascalchi M, Diciotti S, Giannelli M, et al. Progression of brain atrophy in spinocerebellar ataxia type 2: a longitudinal tensor-based morphometry study. PLoS ONE 2014;9:e89410.
13. Brenneis C, Bosch SM, Schocke M, et al. Atrophy pattern in SCA2 determined by voxel-based morphometry. NeuroReport 2003;14:1799–1802.
14. Jacobi H, Reetz K, du Montcel ST, et al. Biological and clinical characteristics of individuals at risk for spinocerebellar ataxia types 1, 2, 3, and 6 in the longitudinal RISCA study: analysis of baseline data. Lancet Neurol 2013;12:650–658.
15. Velazquez-Perez L, Rodriguez-Labrada R, Cruz-Rivas EM, et al. Comprehensive study of early features in spinocerebellar ataxia 2: delineating the prodromal stage of the disease. Cerebellum 2014;13:568–579.
16. Almaguer-Mederos LE, Falcon NS, Almira YR, et al. Estimation of the age at onset in spinocerebellar ataxia type 2 Cuban patients by survival analysis. Clin Genet 2010;78:169–174.
17. Schmitz-Hubsch T, du Montcel ST, Baliko L, et al. Scale for the assessment and rating of ataxia: development of a new clinical scale. Neurology 2006;66:1717–1720.
18. Spreen O, Strauss E. A Compendium of Neuropsychological Tests: administration Norms, and Commentary. New York, NY: Oxford University Press, 1991.
19. Reetz K, Costa AS, Mirzazade S, et al. Genotype-specific patterns of atrophy progression are more sensitive than clinical decline in SCA1, SCA3 and SCA6. Brain 2013;136:905–917.
20. Yushkevich PA, Piven J, Hazlett HC, et al. User-guided 3D active contour segmentation of anatomical structures: significantly improved efficiency and reliability. NeuroImage 2006;31:1116–1128.
21. Rosenthal R. Meta- analytic procedures for social research. (2nd ed). Newbury Park, CA: Sage, 1991.
22. Schols L, Reimold M, Seidel K, et al. No parkinsonism in SCA2 and SCA3 despite severe neurodegeneration of the dopaminergic substantia nigra. Brain 2015;138:3316–3326.
23. Gierga K, Burk K, Bauer M, et al. Involvement of the cranial nerves and their nuclei in spinocerebellar ataxia type 2 (SCA2). Acta Neuropathol 2005;109:617–631.
24. Klockgether T, Skalej M, Wedekind D, et al. Autosomal dominant cerebellar ataxia type I. MRI-based volumetry of posterior fossa structures and basal ganglia in spinocerebellar ataxia types 1, 2 and 3. Brain 1998;121 (Pt 9):1687–1693.
25. Della Nave R, Ginestroni A, Tessa C, et al. Brain white matter tracts degeneration in Friedreich ataxia. An in vivo MRI study using tract-based spatial statistics and voxel-based morphometry. NeuroImage 2008;40:19–25.
26. Oz G, Iltis I, Hutter D, et al. Distinct neurochemical profiles of spinocerebellar ataxias 1, 2, 6, and cerebellar multiple system atrophy. Cerebellum 2011;10:208–217.
27. Guerrini L, Lolli F, Ginestroni A, et al. Brainstem neurodegeneration correlates with clinical dysfunction in SCA1 but not in SCA2. A quantitative volumetric, diffusion and proton spectroscopy MR study. Brain 2004;127:1785–1795.
28. Mandelli ML, De Simone T, Minati L, et al. Diffusion tensor imaging of spinocerebellar ataxias types 1 and 2. AJNR Am J Neuroradiol 2007;28:1996–2000.
29. Della Nave R, Ginestroni A, Tessa C, et al. Brain white matter damage in SCA1 and SCA2. An in vivo study using voxel-based morphometry, histogram analysis of mean diffusivity and tract-based spatial statistics. NeuroImage 2008;43:10–19.
30. Hernandez-Castillo CR, Galvez V, Mercadillo RE, et al. Functional connectivity changes related to cognitive and motor performance in spinocerebellar ataxia type 2. Mov Disord 2015;30:1391–1399.
31. Cocozza S, Sacca F, Cervo A, et al. Modifications of resting state networks in spinocerebellar ataxia type 2. Mov Disord 2015;30:1382–1390.
32. Velazquez-Perez L, Seifried C, Santos-Falcon N, et al. Saccade velocity is controlled by polyglutamine size in spinocerebellar ataxia 2. Ann Neurol 2004;56:444–447.
33. Rodriguez-Labrada R, Velazquez-Perez L, Auburger G, et al. Spinocerebellar ataxia type 2: measures of saccade changes improve power for clinical trials. Mov Disord 2016;31:570–578.

34. Ramat S, Leigh RJ, Zee DS, Optican LM. What clinical disorders tell us about the neural control of saccadic eye movements. Brain 2007;130:10–35.
35. Velazquez-Perez L, Voss U, Rodriguez-Labrada R, et al. Sleep disorders in spinocerebellar ataxia type 2 patients. Neurodegener Dis 2011;8:447–454.
36. Rodriguez-Labrada R, Velazquez-Perez L, Ochoa NC, et al. Subtle rapid eye movement sleep abnormalities in presymptomatic spinocerebellar ataxia type 2 gene carriers. Mov Disord 2011;26:347–350.
37. Tuin I, Voss U, Kang JS, et al. Stages of sleep pathology in spinocerebellar ataxia type 2 (SCA2). Neurology 2006;67:1966–1972.
38. Datta S, Maclean RR. Neurobiological mechanisms for the regulation of mammalian sleep-wake behavior: reinterpretation of historical evidence and inclusion of contemporary cellular and molecular evidence. Neurosci Biobehav Rev 2007;31:775–824.
39. Heller J, Brcina N, Dogan I, et al. Brain imaging findings in idiopathic REM sleep behavior disorder (RBD) - A systematic review on potential biomarkers for neurodegeneration. Sleep Med Rev 2017;34:23–33.
40. Schmahmann JD, Caplan D. Cognition, emotion and the cerebellum. Brain 2006;129:290–292.
41. Rub U, Del Turco D, Del Tredici K, et al. Thalamic involvement in a spinocerebellar ataxia type 2 (SCA2) and a spinocerebellar ataxia type 3 (SCA3) patient, and its clinical relevance. Brain 2003;126:2257–2272.
42. Hoche F, Baliko L, den Dunnen W, et al. Spinocerebellar ataxia type 2 (SCA2): identification of early brain degeneration in one monozygous twin in the initial disease stage. Cerebellum 2011;10:245–253.
43. D'Agata F, Caroppo P, Boghi A, et al. Linking coordinative and executive dysfunctions to atrophy in spinocerebellar ataxia 2 patients. Brain Struct Funct 2011;216:275–288.

